# Structural Properties of Hydration Shell Around Various Conformations of Simple Polypeptides

**Dariusz Czapiewski and Jan Zielkiewicz***

*Gdańsk University of Technology, Department of Chemistry Narutowicza 11/12, 80-952 Gdańsk, Poland*

*Received: September 7, 2009; Revised Manuscript Received: January 20, 2010*

In this paper we investigate structural properties of water within the solvation shell around the peptide core created by a well-defined conformation of polypeptide chain. The following secondary structures are investigated: linear (straight chain), and three helices PII (polyproline-like), $3_{10}$, and α. We propose using the two-particle contribution to entropy as a rational measure of the water structural ordering within the solvation layer. This contribution divides into two terms, depending on the peptide−water and water−water interactions, respectively, and in this paper both terms are investigated. The structure of "solvation" water is described by the second term, and therefore it mainly attracts our attention. Determination of this term, however, is not an easy task, requiring some controversial approximations. Therefore, we have transformed this term to the form of some rational parameter which measures the local structural ordering of water within the solvation shell. Moreover, the results of several independent investigations are reported: we adopt the harmonic approximation for an independent estimation of the water entropy within the solvation shell, and we also study structure of the water−water hydrogen bond network, mean geometry of a single hydrogen bond, the self-diffusion coefficients (both translational and rotational) of water, and the mean lifetimes of water−water and water−peptide hydrogen bonds. All the obtained results lead to the conclusion that the local structure of water within the solvation shell changes only slightly in comparison to the bulk one. If so, the measure of local water ordering proposed by us is exploited with the aim to gain the deeper insight on the structural properties of "solvation" water. It has been shown that this parameter can be factored into three terms, which measure translational, configurational, and orientational ordering, respectively. Using this factoring, the ordering map for a precise description of the water local ordering has been built. An interesting correlation is observed: the points on this map lie approximately on the straight line, while the linear conformations clearly deviate from the general tendency. Further analysis of the obtained results allows us to express the supposition that an increasing local ordering of water around given secondary structure corresponds to an increasing relative stability of this structure in aqueous solution. Analyzing the geometry of the water−water hydrogen bond network within the solvation layer, we find some systematic deviations of this geometry from the bulk water properties. We also observe that the alanine peptides (excluding the linear form) disturb the hydrogen bond network in the less range, and in another way than the various conformations of polyglycine, while the linear form of polyalanine behaves very similarly to the glycine ones. Next, investigating the dynamic properties, we also conclude that water near the peptide surface creates a pseudorigid structure, a "halo" around the peptide core. This "halo" is stabilized by slightly higher energy of the hydrogen bonds network: we have found that within this region the hydrogen bonds network is slightly less distorted, the water−water hydrogen bonds are a little more stable and their mean lifetime is clearly longer that that of bulk water. Significant differences between the alanine- and glycine-based polypeptides are also visible. It has also been found that this solvation layer interacts with the polyalanine in another way than with polyglycine. Although in the case of the glycine-based polypeptide this layer slides relatively freely over the peptide surface, for the alanine-based polypeptide this sliding is strongly hindered by the presence of the methyl groups, and this effect is additionally enhanced by a rise in the solvation layer rigidity. Thus, the survey of various dynamic properties allows us to perceive and to explain distinct differences in behavior of water within the solvation shell around both glycine and alanine peptides.

## Introduction

It is a well-known fact that water plays a crucial role in determining the secondary (tertiary, quaternary) structure of proteins in a solution.[1–3] The influence of the solvent on amino-acid preferences of adopting various secondary structures would account for the fact why prediction of secondary structure is successful in 70% cases only. Also the tendency of various amino acids to create an α-helical structure strongly depends on the solvent.[4,5] An impressive example that illustrates the solvent role is the extreme stability of an unsolvated (in vacuum) α-helical form of polyalanine: it remains almost completely helical up to 725 K, whereas in an aqueous solution the same helix is only marginally stable.[6] To give another persuasive example, we resort to the results obtained by Sorin et al.[7] They showed, by using computer simulations and by manipulation of the Lennard-Jones parameters of water, that the character of

* Corresponding author. E-mail: jaz@chem.pg.gda.pl.

10.1021/jp9086199 
Published on Web 03/16/2010

the solvation interface induces several preferential conformations of the alanine-based polypeptide. Other works also confirm that the solvent environment has a significant effect on the stability of various polyalanine secondary structures.[8,9]

Not only the secondary (tertiary, quaternary) protein structure is solvent dependent but also the protein conformational dynamics (which determines its vital functionality) is tightly connected to the structure and the dynamics of the surrounding water.[10–14] It is even claimed that protein and solvent dynamics are so closely related that they should be perceived as a single entity.[2] It is easy to understand all these facts: the structural stability of a particular peptide conformation is determined by the free energy difference between considered conformational states. The free energy can be divided into two terms: the energetic and the entropic one. To evaluate the influence of the solvent, therefore, we should estimate the solvent dependent contribution to each term. The energetic term may be readily calculated from the simulation data; calculation of the entropic term, however, is a very hard problem. Although the conformational entropy change of the peptide chain can be estimated using, for example, the covariance matrix method,[15–17] the calculation of hydration entropy still remains an unresolved problem, even though its estimation seems to be very important.[18,19] Recently, Lin et al.[20,21] have proposed an approximate method for calculation of the water entropy using the two-phase (2PT) model. This method has been adopted to the entropy calculations of "solvation" water within minor and major grooves of DNA,[22] and as far as we know, this is the only attempt of the local entropy change calculations. We keep in mind that the entropy changes concomitant with the solvation (hydration) process reflect changes in the structure of the surrounding water. These structural changes influence, undoubtedly, many physical properties of water within the solvation layer.[3,10,12] Hence, not only the direct protein−water interactions but also the modification of water structure should be taken into account. In other words, this means that not only water influences the peptide structure but also the structure of the surrounding water "fits" to a particular peptide conformation. Thus, a following question arises: how does the structure (and also various physical properties) of water within the solvation shell around the peptide molecule depend on the given secondary structure formed by this biopolymer? To answer this question, we resort to the concept of *n*-particle correlation functions, which offer a valuable tool for this study. Preliminary results of such studies were reported previously.[23] Now, we extend our investigations onto very important measurements of the solvation layer water−water structural ordering. As far as we know, this is the first attempt of such approach. Moreover, some other methods are also used with the aim of the independent confirmation of our deductions. So, in this paper we present the results of the investigations of some structural and dynamic properties of water within the solvation shell formed around four basic conformations of the polypeptide chain: linear (an extended chain), and three helices: PII (polyproline-like), $3_{10}$, and α.

## Method

**Molecular Dynamics Simulations.** The simulations were carried out using the Amber10[24] molecular dynamics package. Polypeptide ($Ala_{15}$) was built using 15 alanine residues; the Amber ff03 force field was used. Four conformations of the peptide molecule have been investigated: linear (straight chain), and three helices: PII (polyproline-like), $3_{10}$, and α. The peptide molecule was centered within the box; the minimal distance of the peptide molecule from the box walls was 1.5 nm for each conformation. The peptide backbone atoms were positionally restrained (using harmonic forces, $k = 6$ kcal/(mol Å$^2$)) to prevent the conformational changes. For our investigations we use the TIP4P model of water instead of the SPC one used previously.[23] There are two reasons for such a choice. First, we investigate some dynamic properties of water, while the TIP4P model better describes such properties than the SPC one. Second, it is a chance to examine if our deductions depend on the choice of water model.

Besides the peptide−water systems, the system containing only 2410 TIP4P water molecules was also investigated; it has served as a reference system, to determinate the properties of pure water. The simulations of all systems were carried out using *NVT* conditions; the temperature ($T = 298$ K) was kept constant by the weak coupling to an external bath ($\tau_T = 0.2$ ps). Every system was initially equilibrated for at least 2 ns in *NPT* conditions, afterward 0.2 ns in *NVT* conditions, and then the trajectory was written to a file for further analysis.

In this paper we wish to find various properties of the water surrounding a well-defined fragment of the polypeptide secondary structure. Therefore, to avoid the "end effect", two residues at both peptide ends were omitted, and the middle region representing the well-defined structural part of the polypeptide chain was taken into account. So, the analyzed part of the peptide chain is 11 residues long.

**Hydrogen Bond Analysis.** We have adopted the hydrogen bond definition described in the Wernet et al.'s paper.[25] According to this definition, the hydrogen bond between two water molecules is formed if the oxygen−oxygen distance fulfills the relation

$$R_{OO} \leq -0.000044\beta_{OOH}^{\ 2} + 0.33 \text{ [nm]} \qquad (1)$$

where $\beta_{OOH}$ is the O−O−H angle (in degrees). We demanded, moreover, the total interaction energy between two "hydrogen-bonded" molecules to be negative; it is roughly equivalent to demanding that the force acting between these molecules be attractive. This total interaction energy has been calculated as the sum of both Lennard-Jones and electrostatic terms between two molecules for which relation 1 is fulfilled; its absolute value, averaged over all H-bonded molecules, was assumed as the mean H-bond energy of the system. We determine both energy and geometry of the hydrogen bond as a function of the distance *r* from the polypeptide axis.

**Diffusion Coefficients and the Hydrogen Bond Lifetime.** We wish to determine these quantities separately for both the first and the second solvation shell around the peptide molecule. The diffusion coefficients and the lifetimes of the hydrogen bond have been calculated from the appropriate time correlation functions. The following procedures were adopted.

Let $\mathbf{v}_K(t)$ denote a water molecule's vector of translational (K = T), or rotational velocity (K = R). The diffusion coefficients: translational ($D_T$), and rotational ($D_R$), were calculated from the appropriate velocity autocorrelation function using the well-known Green−Kubo relation[26]

$$D_K = \frac{1}{3}\lim_{t\to\infty}\left(\int_0^t C_K(t)\,\mathrm{d}t\right) \qquad (2)$$

where $C_K(t)$ symbolizes the translational (or angular) velocity autocorrelation function:

$$C_K(t) = \lim_{T\to\infty}\left(\frac{1}{T}\int_0^T \mathbf{v}_K(x)\,\mathbf{v}_K(x+t)\,\mathrm{d}x\right) = \langle \mathbf{v}_K(x)\,\mathbf{v}_K(x+t)\rangle \tag{3}$$

Moreover, we decompose the vector $\mathbf{v}_K(t)$ into their components within the "internal" coordinate system of the water molecule. This "internal" coordinate frame (we assume it to be right-handed) originates at the water particle center of mass, and the coordinate axes are the same as the main axes of the inertia tensor; the axes are ordered such that $I_x < I_y < I_z$. Then, the "directional", normalized autocorrelation functions, $C_{K_i}(t)$, have been calculated for each of $i$th component ($i = x, y, z$) of the $\mathbf{v}_K(t)$ vector.

The kinetics of a single hydrogen bond is described by the time correlation function

$$S_A(t) = \langle h(t_0)\,h(t_0+t)\rangle \tag{4}$$

where the binary function $h(t) = 1$ if the investigated hydrogen bond between two water molecules exists continuously (without intermediate breaking) from $t_0$ up to $t$, and $h(t) = 0$ otherwise. In other words, $S_A(t)$ yields the probability that a single hydrogen bond formed at time $t_0$ remains bonded all the time up to $t$. For more details about these calculations, see our previous paper.[23]

**Error Estimation in Diffusion Coefficients and the Hydrogen Bond Lifetimes.** The estimation of obtained results uncertainty is a separate problem, and it is a hard task. We solve this problem by repeating, for all systems, our calculations several (3−5) times, and on this base the error limits for all the investigated quantities have been estimated.

**Two-Particle Contribution to Entropy.** Using the trajectory obtained from the molecular dynamics calculations, the position and orientation of each water molecule were determined; a set of these quantities reflects the internal structure of water in the vicinity of the peptide. To obtain a precise description, we need some measure of that structural ordering, and the absolute entropy of water can serve as such a measure. However, calculations of this quantity are a very hard task. We resort to the Green concept, which allows us to decompose the total system entropy into the $n$-particle contributions. The entropy of an $N$-particle system can be calculated as a sum of the series

$$S = s^{\mathrm{id}} + s^{(2)} + s^{(3)} + \ldots + s^{(N)} = s^{\mathrm{id}} + s^{\mathrm{exc}} \tag{5}$$

where $s_{\mathrm{id}}$ symbolizes the entropy of an ideal gas and $s^{(n)}$ describes the contributions to the entropy originating from an $n$-particle correlation ($n = 2, 3, \ldots, N$). This expression was first derived by Green;[27] later, Nettleton and Green,[28] and much later also Raveché,[29] obtained a similar expansion for the entropy of open systems, and this idea has been followed by many authors.[30−36] This method allows us to calculate the absolute entropy of the system; however, it is difficult, or even impossible, to determine the $n$-particle correlation functions for higher $n$ ($n > 2$). Therefore, the higher terms in series (5) are omitted in practice—this is the so-called two-particle approximation. Within this approximation, the expression for the entropy reduces to the form

$$S \cong s^{\mathrm{id}} + s^{(2)} \tag{6}$$

For the peptide−water binary mixture term $s_{\mathrm{id}}$ can be expressed by the relation

$$s^{\mathrm{id}} = N_{\mathrm{P}}s_{\mathrm{P}}^{\mathrm{id}} + N_{\mathrm{W}}s_{\mathrm{W}}^{\mathrm{id}} = N_{\mathrm{P}}\left\{3k_{\mathrm{B}} - k_{\mathrm{B}}\ln\left[\frac{\rho_{\mathrm{P}}\sigma_{\mathrm{P}}}{\Omega}\lambda_{\mathrm{TP}}{}^3\,\lambda_{\mathrm{RP}}\right]\right\} + N_{\mathrm{W}}\left\{3k_{\mathrm{B}} - k_{\mathrm{B}}\ln\left[\frac{\rho_{\mathrm{W}}\sigma_{\mathrm{W}}}{\Omega}\lambda_{\mathrm{TW}}{}^3\,\lambda_{\mathrm{RW}}\right]\right\} \tag{7}$$

where indexes P and W denote protein and water, respectively, $N$ represents the total number of molecules, $\rho$ is the number density ($\rho = N/V$, $V$ is the volume of system), $\sigma$ is the symmetry number (for water $\sigma_{\mathrm{W}} = 2$, for peptide, in general, $\sigma_{\mathrm{P}} = 1$). The other symbols are

$$\lambda_{\mathrm{T}} = \frac{h}{\sqrt{2\pi m k_{\mathrm{B}}T}} \qquad \lambda_{\mathrm{R}} = \left(\frac{h}{\sqrt{2\pi k_{\mathrm{B}}T}}\right)^3\cdot\frac{1}{\sqrt{I_xI_yI_z}} \qquad \Omega = 8\pi^2 \tag{8}$$

where $I$ symbolizes a molecule's main moments of inertia, $m$ is its mass, and $h$ and $k_{\mathrm{B}}$ represent Planck and Boltzmann constants, respectively. The two-particle contribution to entropy for such two-component system has the form[34,36]

$$\begin{aligned} s^{(2)} = &-\frac{\rho_{\mathrm{P}}{}^2}{2!\Omega^2}k_{\mathrm{B}}\int\{g_{\mathrm{PP}}^{(2)}(\mathbf{r}_{\mathrm{P1}},\mathbf{r}_{\mathrm{P2}},\boldsymbol{\omega}_{\mathrm{P1}},\boldsymbol{\omega}_{\mathrm{P2}})\\ &\ln[g_{\mathrm{PP}}^{(2)}(\mathbf{r}_{\mathrm{P1}},\mathbf{r}_{\mathrm{P2}},\boldsymbol{\omega}_{\mathrm{P1}},\boldsymbol{\omega}_{\mathrm{P2}})] - g_{\mathrm{PP}}^{(2)}(\mathbf{r}_{\mathrm{P1}},\mathbf{r}_{\mathrm{P2}},\boldsymbol{\omega}_{\mathrm{P1}},\boldsymbol{\omega}_{\mathrm{P2}}) + 1\}\\ &\mathrm{d}\mathbf{r}_{\mathrm{P1}}\,\mathrm{d}\mathbf{r}_{\mathrm{P2}}\,\mathrm{d}\boldsymbol{\omega}_{\mathrm{P1}}\,\mathrm{d}\boldsymbol{\omega}_{\mathrm{P2}} - \frac{\rho_{\mathrm{P}}\rho_{\mathrm{W}}}{2!\Omega^2}k_{\mathrm{B}}\int\{g_{\mathrm{PW}}^{(2)}(\mathbf{r}_{\mathrm{P}},\mathbf{r}_{\mathrm{W}},\boldsymbol{\omega}_{\mathrm{P}},\boldsymbol{\omega}_{\mathrm{W}})\\ &\ln[g_{\mathrm{PW}}^{(2)}(\mathbf{r}_{\mathrm{P}},\mathbf{r}_{\mathrm{W}},\boldsymbol{\omega}_{\mathrm{P}},\boldsymbol{\omega}_{\mathrm{W}})] - g_{\mathrm{PW}}^{(2)}(\mathbf{r}_{\mathrm{P}},\mathbf{r}_{\mathrm{W}},\boldsymbol{\omega}_{\mathrm{P}},\boldsymbol{\omega}_{\mathrm{W}}) + 1\}\\ &\mathrm{d}\mathbf{r}_{\mathrm{P}}\,\mathrm{d}\mathbf{r}_{\mathrm{W}}\,\mathrm{d}\boldsymbol{\omega}_{\mathrm{P}}\,\mathrm{d}\boldsymbol{\omega}_{\mathrm{W}} - \frac{\rho_{\mathrm{W}}{}^2}{2!\Omega^2}k_{\mathrm{B}}\int\{g_{\mathrm{WW}}^{(2)}(\mathbf{r}_{\mathrm{W1}},\mathbf{r}_{\mathrm{W2}},\boldsymbol{\omega}_{\mathrm{W1}},\boldsymbol{\omega}_{\mathrm{W1}})\\ &\ln[g_{\mathrm{WW}}^{(2)}(\mathbf{r}_{W1},\mathbf{r}_{\mathrm{W2}},\boldsymbol{\omega}_{\mathrm{W1}},\boldsymbol{\omega}_{\mathrm{W2}})] - g_{\mathrm{WW}}^{(2)}(\mathbf{r}_{\mathrm{W1}},\mathbf{r}_{\mathrm{W2}},\boldsymbol{\omega}_{\mathrm{W1}},\boldsymbol{\omega}_{\mathrm{W2}}) + 1\}\\ &\mathrm{d}\mathbf{r}_{\mathrm{W1}}\,\mathrm{d}\mathbf{r}_{\mathrm{W2}}\,\mathrm{d}\boldsymbol{\omega}_{\mathrm{W1}}\,\mathrm{d}\boldsymbol{\omega}_{\mathrm{W2}} = s_{\mathrm{PP}}^{(2)} + s_{\mathrm{PW}}^{(2)} + s_{\mathrm{WW}}^{(2)} \end{aligned} \tag{9}$$

where $g^{(2)}$ symbolizes the two-particle correlation function, depending on the space positions $\mathbf{r}$ and the orientations $\boldsymbol{\omega}$ of both regarded molecules. The integrals are calculated over accessible positions and orientations of all molecular pairs. Now we wish to exploit the above relation for estimation of the water entropy around the various conformations of the polypeptide chain. Using this relation requires, however, some care. Therefore, each of the terms, $s_{\mathrm{PP}}^{(2)}$, $s_{\mathrm{PW}}^{(2)}$, and $s_{\mathrm{WW}}^{(2)}$, will be considered by us separately. Subsections a and b presented below describe our argument.

(a) At the beginning, we note that the first term in relation 9, $s_{\mathrm{PP}}^{(2)}$, describes the peptide−peptide interactions, and therefore it is out of our interest. The second term in this expression, $s_{\mathrm{PW}}^{(2)}$, describes the protein−water interactions. It depends on twelve variables in summary. If the investigated system, however, is homogeneous and isotropic (translation and rotation invariant), the number of variables reduces to six, and this term is equal to

$$s_{\mathrm{PW}}^{(2)} = -N_{\mathrm{P}}k_{\mathrm{B}}\frac{\rho_{\mathrm{W}}}{2!\Omega}\int[g_{\mathrm{PW}}^{(2)}(\mathbf{r},\boldsymbol{\omega})\ln g_{\mathrm{PW}}^{(2)}(\mathbf{r},\boldsymbol{\omega}) - g_{\mathrm{PW}}^{(2)}(\mathbf{r},\boldsymbol{\omega}) + 1]\,\mathrm{d}\mathbf{r}\,\mathrm{d}\boldsymbol{\omega} \tag{10}$$

where $\mathbf{r}$ and $\boldsymbol{\omega} = (\alpha, \beta, \gamma)$ denote the position and the three Euler angles, which determine position and orientation of a water molecule relative to the peptide one. Moreover, we assume, for

simplicity, that the investigated fragment of the secondary structure formed by the polypeptide chain has a cylindrical symmetry. Under this assumption, we need only four variables: the distance $r$ of the water molecule (as its center of mass) from the peptide axis, and the three Euler angles, $\boldsymbol{\omega} = (\alpha, \beta, \gamma)$, describing its orientation relative to this axis. Definitions of these variables are the same as in our previous paper.[23] For the description of such ordering, we determine the function $g^{(2)}_{PW}(r,\alpha,\beta,\gamma) = g^{(2)}_{PW}(r,\boldsymbol{\omega})$, defined in the cylindrical coordinates as follows

$$g^{(2)}_{PW}(r,\boldsymbol{\omega}) = \frac{\Omega}{\rho_W}\frac{dN(r,\boldsymbol{\omega})}{dV\,d\boldsymbol{\omega}} = \frac{\Omega}{\rho_W}\frac{dN(r,\boldsymbol{\omega})}{2\pi r L dr\,d\boldsymbol{\omega}} \quad (11)$$

where $L$ symbolizes the cylinder length, $dN(r,\boldsymbol{\omega})$ denotes the number of water particles that are present within the distance range $(r,r+dr)$ and that are orientated within the range $(\boldsymbol{\omega},\boldsymbol{\omega}+d\boldsymbol{\omega})$, and

$$d\boldsymbol{\omega} = \sin\alpha\, d\alpha\, d\beta\, d\gamma \qquad \Omega = \int d\boldsymbol{\omega} = 8\pi^2$$
$$0 \le \alpha < \pi \qquad 0 \le \beta < 2\pi \qquad 0 \le \gamma < 2\pi \quad (12)$$

Function 11 describes the probability distribution, relative to a completely random one, of the water molecule found at a given distance $r$ from the peptide axis, and at the given orientation $(\alpha, \beta, \gamma)$ relative to this axis. After integration of this function, we can find the familiar radial distribution function, $g(r)$ (here expressed in cylindrical coordinates), or some other functions describing the probability distribution of each of the Euler angles at a given distance $r$.

In our previous paper we proposed (following the idea first described by Lazaridis and Karplus[37]) to use the orientational part, $s^{(2)}_{PW,orient}$, of the two-particle contribution to entropy, $s^{(2)}_{PW}$, as the measure of the water structural ordering within the solvation layer around peptide core. A mathematical expression for $s^{(2)}_{PW,orient}$ may be obtained as follows.

Using the method described previously,[38,39] the distribution function, $g^{(2)}_{PW}(r,\boldsymbol{\omega})$, can be factored as

$$g^{(2)}_{PW}(r,\boldsymbol{\omega}) = \frac{V\Omega}{N}\frac{dN(r,\boldsymbol{\omega})}{dV\,d\boldsymbol{\omega}} = \frac{V}{N}\frac{dN(r)}{dV}\frac{\Omega}{dN(r)}\frac{dN(r,\boldsymbol{\omega})}{d\boldsymbol{\omega}} = g(r)\cdot g^{(2)}_{orient}(r,\boldsymbol{\omega}) \quad (13)$$

where we define

$$g(r) = \frac{V}{N}\frac{dN(r)}{dV} = \frac{1}{\rho_W}\frac{dN(r)}{2\pi L r\,dr} \qquad \text{and} \qquad g^{(2)}_{orient}(r,\boldsymbol{\omega}) = \frac{\Omega}{dN(r)}\frac{dN(r,\boldsymbol{\omega})}{d\boldsymbol{\omega}} \quad (14)$$

Both of these functions, $g(r)$ and $g^{(2)}_{orient}(r,\boldsymbol{\omega})$, fulfill the obvious normalization conditions:

$$\frac{1}{V}\int g(r)\,dV = 1 \qquad \text{and} \qquad \frac{1}{\Omega}\int g^{(2)}_{orient}(r,\boldsymbol{\omega})\,d\boldsymbol{\omega} = 1 \quad (15)$$

Inserting relations 14 into eq 10, after considerable algebra we find

$$s^{(2)}_{PW} = -N_P k_B \frac{\rho_W}{2!}\int (I_{trans}(r) + I_{orient}(r))\,dV = s^{(2)}_{PW,trans} + s^{(2)}_{PW,orient} \quad (16)$$

where

$$I_{trans}(r) = g(r)\ln g(r) - g(r) + 1$$
$$I_{orient}(r) = \frac{g(r)}{\Omega}\int g^{(2)}_{orient}(r,\boldsymbol{\omega})\ln g^{(2)}_{orient}(r,\boldsymbol{\omega})\,d\boldsymbol{\omega} \quad (17)$$

and

$$s^{(2)}_{PW,trans} = -N_P k_B \frac{\rho_W}{2!}\int I_{trans}(r)\,dV = -N_P k_B \rho_W L\pi \int_0^\infty I_{trans}(r) r\,dr$$
$$s^{(2)}_{PW,orient} = -N_P k_B \frac{\rho_W}{2!}\int I_{orient}(r)\,dV = -N_P k_B \rho_W L\pi \int_0^\infty I_{orient}(r) r\,dr \quad (18)$$

Thus, the $s^{(2)}_{PW,orient}$ value can serve as a rational measure of the water structural ordering relative to the peptide core. This measure has the following characteristic properties. For all $r < R_c$ ($R_c$ is the radius of peptide core) we have, of course, $g^{(2)}_{PW}(r,\boldsymbol{\omega}) = 0$, so in this region $s^{(2)}_{PW,orient} = 0$. If $r > R_c$, and for a completely random distribution we have (by definition) $g^{(2)}_{PW}(r,\boldsymbol{\omega}) = 1$, and therefore we also read $s^{(2)}_{PW,orient} = 0$. On the other hand, an increasing ordering of water molecules produces smaller and smaller (negative) values of $s^{(2)}_{PW,orient}$, and for an ideal, crystal-like arrangement this value goes (as it may easily be shown) to minus infinity. Moreover, by integration of $I_{orient}(r)$ within the $(0, r)$ interval we obtain the $s^{(2)}_{PW,orient}(r)$ function:

$$s^{(2)}_{PW,orient}(r) = -N_P k_B \frac{\rho_W}{2!}\int_0^r I_{orient}(r)\,dV = -N_P k_B \rho_W L\pi \int_0^r I_{orient}(r) r\,dr \quad (19)$$

The function $I_{orient}(r)$ contains information about orientational effects present at distance $r$, while the function $s^{(2)}_{PW,orient}(r)$ measures a local orientational ordering of water in the surrounding space at the distance up to $r$. This allows us to estimate, in a rational manner, both the scope and the magnitude of the water structural ordering around the peptide core. Note that all these remarks may also be adapted, of course, to the $s^{(2)}_{PW,orient}$ contribution, which describes a translational ordering of water around the peptide, and to the $s^{(2)}_{PW}$ quantity.

(b) A similar role, as a measure of structural ordering, is played by the last term in eq 9. It depends on the water−water interactions, and therefore its value serves as the measure of the water structural ordering in the vicinity of the peptide surface. So, it is highly desired that its estimation be done. Calculation of this term is, however, very difficult, because in the vicinity of the peptide the two-particle correlation function, $g^{(2)}_{WW}$, depends on all twelve variables. For a given pair of water molecules, these variables describe the position and the orientation of the each one relative to the peptide core. So, it seems that (accurate) determination of the third term in integral 9 is, up to today, quite impossible in practice, and several approximations are required. Thus, our argument is as follows.

At first, we take into account the water molecules belonging to both the first and the second solvation layer around investigated part of the polypeptide core; these are the central ones. This space region represents a drilled cylinder of outer radius $R_{sol}$ around the investigated peptide core. Now, we assume this region to be homogeneous, and under this assumption the contribution $g^{(2)}_{WW}$ transforms to

$$s^{(2)}_{WW} = -N_W k_B \frac{\rho_W}{2\Omega_2} \int \{g^{(2)}_{WW}(r,\boldsymbol{\omega}_1,\boldsymbol{\omega}_2) \ln[g^{(2)}_{WW}(r,\boldsymbol{\omega}_1,\boldsymbol{\omega}_2)] - g^{(2)}_{WW}(r,\boldsymbol{\omega}_1,\boldsymbol{\omega}_2) + 1\} r^2 \, dr \, d\boldsymbol{\omega}_1 \, d\boldsymbol{\omega}_2 \quad (20)$$

where $r$ and $\boldsymbol{\omega}_1 = (\varphi, \theta)$ represent the distance and the two angles (in a spherical coordinate system) describing the position of a surrounding water molecule relative to the central one, while $\boldsymbol{\omega}_2 = (\alpha, \beta, \gamma)$ symbolizes the three Euler angles determining orientation of a surrounding water particle relative to the central one. Thus, a set of six variables, $(r, \boldsymbol{\omega}_1, \boldsymbol{\omega}_2)$, describes relative position and orientations of two water molecules. We have, of course

$$\begin{aligned} &d\boldsymbol{\omega}_1 = \sin\theta \, d\varphi \, d\theta \qquad d\boldsymbol{\omega}_2 = \sin\alpha \, d\alpha \, d\beta \, d\gamma \\ &\Omega_1 = \int d\boldsymbol{\omega}_1 = 4\pi \qquad \Omega_2 = \int d\boldsymbol{\omega}_2 = 8\pi^2 \\ &\text{where} \quad 0 < r < \infty \quad 0 < \varphi < 2\pi \quad 0 < \theta < \pi \\ &0 < \alpha < \pi \quad 0 < \beta < 2\pi \quad 0 < \gamma < 2\pi \end{aligned} \quad (21)$$

In other words, the computed (under above assumption) $s^{(2)}_{WW}$ value can serve as some averaged measure of the structural ordering of water molecules within the solvation layer of the radius $R_{sol}$. The use of the $s^{(2)}_{WW}$ contribution as a measure of water structural ordering has already been suggested by Truskett et al.,[40] and recently it has also been successfully adopted by Esposito et al.[41] for a description of the overall ordering in liquid water under various $p-3T$ conditions. Now, we want to exploit this idea to the description of *local structural ordering* of water within solvation layer.

Our reasoning is the following. As shown previously,[38,39] it is possible to calculate the function $s^{(2)}_{WW}(r)$, which measures the local ordering of water in the surrounding space at the distances up to $r$. On the other hand, from our previous paper[39] it follows that (in pure water) the scope of the local ordering does not exceed 0.58 nm, while the first solvation shell around a water particle (at distances $r < 0.35$ nm) contributes roughly in 70% to the total orientational effects. In other words, the following numerical values of the $s^{(2)}_{WW}$ quantity were calculated at two mentioned distances:

$$s^{(2)}_{WW}(r = 0.35 \text{ nm}) \qquad \text{and} \qquad s^{(2)}_{WW}(r = 0.58 \text{ nm}) \quad (22)$$

The *local ordering* in pure liquid water is measured in the limits of the first and second hydration layers around the water molecule. Then we propose here to use the above quantities (22) as a measure of the *average local ordering* of water within the solvation layer around the peptide core. In this paper we use the value 0.36 nm instead of the one estimated previously equal to 0.35 nm, because the integration step $\Delta r = 0.02$ nm (the same as in ref 39) has been used.

Moreover, it is possible to factor the function $g^{(2)}_{WW}$ into three terms, which we call the translational, configurational, and orientational ones.[39] This factoring was made in a way quite similar to the one described above for factoring $g^{(2)}_{WW}$. We read

$$\begin{aligned} g^{(2)}_{WW}(r,\boldsymbol{\omega}) &= \frac{V\Omega_2}{N} \frac{dN(r,\boldsymbol{\omega}_1,\boldsymbol{\omega}_2)}{r^2 \, dr \, d\boldsymbol{\omega}_1 \, d\boldsymbol{\omega}_2} = \left(\frac{V}{N} \frac{dN(r)}{\Omega_1 r^2 \, dr}\right) \cdot \\ &\left(\frac{\Omega_1}{dN(r)} \frac{dN(r,\boldsymbol{\omega}_1)}{d\boldsymbol{\omega}_1}\right) \cdot \left(\frac{\Omega_2}{dN(r,\boldsymbol{\omega}_1)} \frac{dN(r,\boldsymbol{\omega}_1,\boldsymbol{\omega}_2)}{d\boldsymbol{\omega}_2}\right) \\ &= g^{(2)}_r(r) \cdot g^{(2)}_{conf}(r,\boldsymbol{\omega}_1) \cdot g^{(2)}_{orient}(r,\boldsymbol{\omega}_1,\boldsymbol{\omega}_2) \end{aligned} \quad (23)$$

where we define

$$\begin{aligned} g^{(2)}_r(r) &= \frac{V}{N} \frac{dN(r)}{\Omega_1 r^2 \, dr} = \frac{V}{N} \frac{dN(r)}{dV(r)} \\ g^{(2)}_{conf}(r,\boldsymbol{\omega}_1) &= \frac{\Omega_1}{dN(r)} \frac{dN(r,\boldsymbol{\omega}_1)}{d\boldsymbol{\omega}_1} \\ g^{(2)}_{orient}(r,\boldsymbol{\omega}_1,\boldsymbol{\omega}_2) &= \frac{\Omega_2}{dN(r,\boldsymbol{\omega}_1)} \frac{dN(r,\boldsymbol{\omega}_1,\boldsymbol{\omega}_2)}{d\boldsymbol{\omega}_2} \end{aligned} \quad (24)$$

Inserting relations 24 into eq 20, after considerable algebra, it is easy to find the final result: the contribution $s^{(2)}_{WW}(r)$ becomes the sum of three terms

$$s^{(2)}_{WW}(r) = s^{(2)}_{WW,trans}(r) + s^{(2)}_{WW,conf}(r) + s^{(2)}_{WW,orient}(r) \quad (25)$$

where

$$\begin{aligned} s^{(2)}_{WW,trans}(r) &= -\frac{\rho_W N_W k_B}{2!} \int_0^r I_{trans}(r) 4\pi r^2 \, dr \\ I_{trans}(r) &= g^{(2)}_r(r) \ln[g^{(2)}_r(r)] - g^{(2)}_r(r) + 1 \\ s^{(2)}_{WW,conf}(r) &= -\frac{\rho_W N_W k_B}{2!} \int_0^r I_{conf}(r) 4\pi r^2 \, dr \\ I_{conf}(r) &= \frac{g^{(2)}_r(r)}{\Omega_1} \int g^{(2)}_{conf}(r,\boldsymbol{\omega}_1) \ln[g^{(2)}_{conf}(r,\boldsymbol{\omega}_1)] \, d\boldsymbol{\omega}_1 \\ s^{(2)}_{WW,orient}(r) &= -\frac{\rho_W N_W k_B}{2!} \int_0^r I_{orient}(r) 4\pi r^2 \, dr \\ I_{orient}(r) &= -\frac{g^{(2)}_r(r)}{\Omega_1 \Omega_2} \int g^{(2)}_{conf}(r,\boldsymbol{\omega}_1) \, g^{(2)}_{orient}(r,\boldsymbol{\omega}_1,\boldsymbol{\omega}_2) \\ &\quad \ln[g^{(2)}_{orient}(r,\boldsymbol{\omega}_1,\boldsymbol{\omega}_2)] \, d\boldsymbol{\omega}_1 \, d\boldsymbol{\omega}_2 \end{aligned} \quad (26)$$

The values of each of these terms were also determined at both (0.36 and 0.58 nm) distances. From the above relations it is also easy to see that the configurational term, $s^{(2)}_{WW,conf}(r)$, measures the local ordering of surrounding water molecules (treated as points) around the central one. Note that its determination is significantly less labor-consuming than determination of $s^{(2)}_{WW,conf}(r)$ and $s^{(2)}_{WW}(r)$ ones. Therefore, in our opinion this term can serve as a rational measure of such ordering, instead of the well-known empirical Chau and Hardwick's[42] "tetrahedral ordering" parameter. We return to this concept in the Results and Discussion.

**Technical Details of Calculations.** For calculations of the integrals given by eqs 18−20, the following steps of integration were used: $\Delta r = 0.02$ nm and $\Delta\alpha = 10°$ for all angles. The

total simulation time for these calculations was equal to 16−20 ns, the trajectory was written to the file after each 0.008 ps. The results of the two-particle contributions to entropy computed from the set of trajectories were saved (as a function of the simulation time) after each 1.6 ns. Then, these intermediate results were extrapolated to an "infinitely long" simulation. As found previously,[38] the following function

$$S^{(2)}(t) = S_\infty - \frac{A}{B + \sqrt{t}(\ln t + C)} \tag{27}$$

excellently fits the entropy results as a function of the simulation time, $t$. In the above relation $S_\infty$ symbolizes the entropy in the limit $t \rightarrow \infty$; $S_\infty$, $A$, $B$, and $C$ are adjustable parameters determined using the Marquardt[43] (least-squares) method.

## Results and Discussion

As mentioned in the Method section, all the discussed results describe various properties of water around a well-defined secondary structure, formed by the middle region of the peptide chain. For more clarity, our argument is divided into five subsections, (a)−(e), which describe (in some logical sequence) the obtained results. So, in subsections a and b we investigate structural properties of water within the solvation layer, and we introduce a measure of local structural ordering of water. In subsection c we scrutinize some properties of the hydrogen bond network, while in subsection d some dynamic properties are investigated; we also link them with the structural ones. The last subsection (e) describes interaction of the solvation layer with the peptide core.

(a) At the beginning, we wish to survey the course of the $g(r)$ curve (defined by eq 14), presented in Figure 1a for all the investigated structures of the polyalanine chain. It allows us to estimate the radius of the solvation layer around the peptide core. In contrast with the results obtained previously for the glycine-based polypeptide,[23] we observe multiple peaks, which reflect the complicated structure of the first solvation layer around the polyalanine. For two forms of the peptide chain (linear and α-helix) the detailed analysis has been performed. As in the results, the particular peaks have been ascribed as follows (see Figure 1b,c for illustration). The peak denoted HB reflects interactions between water molecules and the carbonyl group oxygen atom, while the peaks denoted CA and CB reflect the hydration of the backbone CH group and the side group ($CH_3$), respectively. On the other hand, the observed relative deep minimum at 0.76 nm (for the α-helix) and 0.64 nm (for the linear form) reflects a border between the first and the second solvation layers. The thickness of both these layers can be approximately estimated equal to 0.4 nm for the first, and 0.3 nm for the second one. Note that the first solvation layer cannot be defined very well, because of the presence of side $CH_3$ groups. The thickness of each layer roughly corresponds to the diameter of a single water molecule. Thus in Figure 1, the observed course of the $g(r)$ curve strongly suggests that the space surrounding the peptide core can be divided into two solvation shells: the first and the second one. No more layers are observed. We conclude, therefore, that the scope of solvation effects does not exceed 0.65−0.70 nm approximately (two solvation layers).

To describe the orientational effects of water molecules toward the peptide core, we use the $s^{(2)}_{PW}$ term in eq 9. The general picture is very similar to the one obtained previously for the glycine-based polypeptide.[23] Therefore, only final numerical results are collected in Table 1. For comparison purposes, the

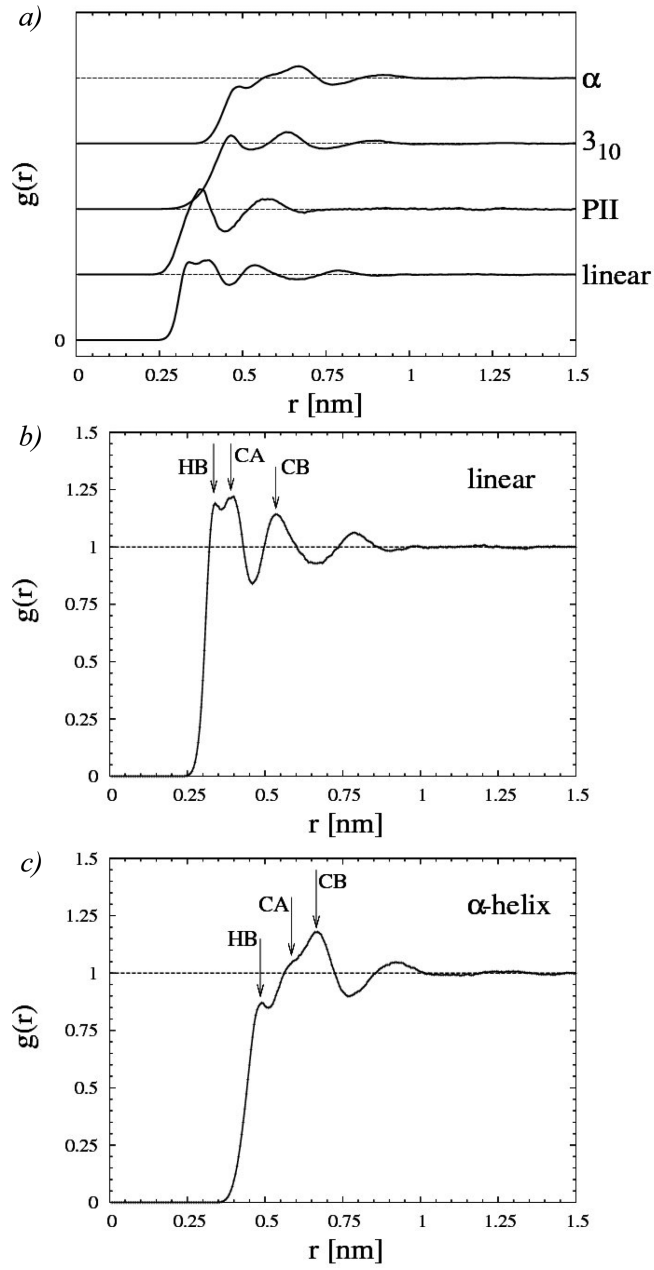


**Figure 1.** (a) Radial distribution functions determined for various conformations of the polyalanine chain. The distribution functions for various structures have been displaced vertically for more clarity. (b) and (c) description of particular peaks on the radial distribution function for both the linear and α-helix conformations.

results for polyglycine are also included. Note that results for polyglycine are *not* the same as in our previous paper. To avoid the effect of various force fields, we do not use the previous results, but we repeat these calculations using the same force field (Amber ff03) and the same water model (TIP4P) as for polyalanine. We can say that the values of the $s^{(2)}_{PW}$ term are generally similar for both polyalanine and polyglycine and differences reflect the presence of the hydrophobic $CH_3$ group in alanine. Note, moreover, that the second solvation layer around the polyalanine is significantly less distinct than the one around the polyglycine.

(b) Now, we wish to investigate the $s^{(2)}_{WW}(r)$ term, which describes the structure of water within the solvation layer. As described in the Method section, this quantity decomposes into three terms (see eq 25), and we determine two values of each

**TABLE 1: Values of $S_{tra}(r) = s^{(2)}_{PW,trans}(r)$, $S_{ort}(r) = s^{(2)}_{PW,orient}(r)$ and $S^{(2)}(r) = s^{(2)}_{PW}(r)$ Calculated at Limits of the first ($R_1$) and the Second ($R_2$) Solvation Layers around the Peptide Core[a]**

| | $R_1$ [nm] | $S_{tra}(R_1)$ | $S_{ort}(R_1)$ | $S^{(2)}(R_1)$ | $R_2$ [nm] | $S_{tra}(R_2)$ | $S_{ort}(R_2)$ | $S^{(2)}(R_2)$ |
|---|---|---|---|---|---|---|---|---|
| Alin | 0.64 | −273.7 | −131.6 | −402.2 | 0.95 | −274.9 | −132.9 | −403.7 |
| APII | 0.68 | −241.6 | −191.9 | −433.5 | 0.90 | −241.8 | −193.7 | −436.0 |
| A310 | 0.74 | −255.6 | −111.4 | −368.2 | 1.05 | −256.2 | −112.2 | −368.4 |
| Aα | 0.76 | −265.4 | −148.9 | −416.5 | 1.10 | −266.4 | −151.9 | −419.8 |
| Glin | 0.54 | −321.3 | −122.6 | −439.7 | 0.90 | −325.2 | −135.2 | −455.4 |
| GPII | 0.58 | −230.2 | −122.4 | −352.6 | 0.86 | −233.1 | −127.0 | −361.1 |
| G310 | 0.64 | −206.8 | −110.8 | −317.6 | 0.97 | −210.1 | −115.0 | −325.1 |
| Gα | 0.69 | −254.5 | −115.0 | −369.5 | 1.00 | −259.0 | −120.2 | −379.2 |

[a] All the values are given in J/(mol K) units.

**TABLE 2: Values of $S(r)$ (Defined by Eq 28) Calculated for the Investigated Systems[a] and Values of Each Term in Eq 25[,b]**

(a) $S(r)$ (Defined by Eq 28)

| | $R_{sol}$ [nm] | $N_W$ | $S(0.36)$ | $S(0.58)$ | $\Delta S(0.36)$ | $\Delta S(0.58)$ | $S_H$ | $\Delta S_H$ |
|---|---|---|---|---|---|---|---|---|
| Alin | 0.95 | 334 | 81.60 | 69.89 | 1.72 | 1.84 | 68.45 | −0.08 |
| APII | 0.90 | 253 | 81.29 | 69.45 | 1.50 | 1.89 | 68.40 | −0.13 |
| A310 | 1.05 | 227 | 80.88 | 68.84 | 1.09 | 1.28 | 68.54 | −0.01 |
| Aα | 1.10 | 193 | 80.70 | 68.60 | 0.91 | 1.06 | 68.44 | −0.09 |
| Glin | 0.90 | 309 | 81.53 | 70.21 | 1.74 | 2.65 | 68.48 | −0.05 |
| GPII | 0.86 | 232 | 81.86 | 70.44 | 2.07 | 2.88 | 68.52 | −0.01 |
| G310 | 0.97 | 196 | 81.61 | 70.01 | 1.82 | 2.45 | 68.58 | 0.05 |
| Gα | 1.00 | 159 | 81.40 | 69.81 | 1.61 | 2.25 | 68.65 | 0.12 |
| bulk water | | | 79.79 | 67.56 | 0.00 | 0.00 | 68.53 | 0.00 |

(b) Values of Each Term in Eq 25

| | $r = 0.36$ nm | | | $r = 0.58$ nm | | |
|---|---|---|---|---|---|---|
| | $s^{(2)}_{WW,trans}/N_W$ | $s^{(2)}_{WW,conf}/N_W$ | $s^{(2)}_{WW,orient}/N_W$ | $s^{(2)}_{WW,trans}/N_W$ | $s^{(2)}_{WW,conf}/N_W$ | $s^{(2)}_{WW,orient}/N_W$ |
| Alin | −12.14 | −11.22 | −23.88 | −12.65 | −13.41 | −32.80 |
| APII | −12.11 | −11.24 | −24.07 | −12.85 | −13.36 | −33.10 |
| A310 | −12.19 | −11.33 | −24.35 | −12.89 | −13.46 | −33.56 |
| Aα | −12.20 | −11.38 | −24.47 | −12.93 | −13.51 | −33.69 |
| Glin | −12.14 | −11.14 | −23.93 | −12.55 | −13.36 | −32.63 |
| GPII | −12.06 | −11.06 | −23.79 | −12.64 | −13.23 | −32.43 |
| G310 | −12.13 | −11.14 | −23.64 | −12.73 | −13.31 | −32.71 |
| Gα | −12.14 | −11.16 | −24.01 | −12.83 | −13.32 | −32.82 |
| bulk water | −12.16 | −11.31 | −25.49 | −12.37 | −13.61 | −35.21 |

[a] $R_{sol}$ symbolizes the outer radius of space region around the peptide core, $N_W$ represents mean number of water molecules within this region, $S_H$ is the entropy calculated using Henchman's method (also recalculated per one water molecule). $\Delta S$ and $\Delta S_H$ describe the deviation of the appropriate value from the one for bulk water (bulk water properties are given in the last line of the table). All values are given in J/(mol K) units. [b] Recalculated per one water molecule and determined at two values of $r$: 0.36 and 0.58 nm (see text). The last line of the table contains results for bulk water. All the values are given in J/(mol K) units.

of these terms, calculated at the distances: $r = 0.36$ nm and $r = 0.58$ nm. According to the previously presented argument, the $s^{(2)}_{WW}(r)$ value measures, at the given $r$, the local ordering of water at the distance up to $r$, while $s^{(2)}_{WW,trans}(r)$, $s^{(2)}_{WW,trans}(r)$, and $s^{(2)}_{WW,trans}(r)$ measure the translational, configurational, and orientational contributions to this local ordering. Now, we use the value

$$S(r) = s^{id}_{WW} + \frac{s^{(2)}_{WW}(r)}{N_W} \tag{28}$$

instead of $s^{(2)}_{WW}(r)$ one, where $s^{id}_{WW} = 128.75$ J/(mol K) for TIP4P model (see eqs 7 and 8), and $N_W$ denotes the number of water particles within the investigated region of the solvation shell around the peptide core. So, the physical meaning of the $S(r)$ quantity is as follows: it represents the value of a two-particle entropy calculated at the distance up to $r$, recalculated per one water molecule. The results of our calculations are collected in Table 2a, and they can be shortly summarized as follows. First, the $S(r)$ values increase in comparison to the ones for bulk water. Second, these differences are relatively small.

Especially the first conclusion seems to be unexpected. It suggests that the water around the peptide core is (locally) *less* ordered (less structured) than the bulk one. We remember, however, that the controversial assumption was made under the derivation of eq 20. Therefore, any independent method for the entropy calculation is highly desired. Recently Henchman[44,45] proposed a simple method for estimation of the absolute entropy of pure water, using the harmonic approximation. This method is based on the calculation of the mean force (or torque) acting on a single water molecule, and therefore it is also sensitive to water structure. After a slight modification of this procedure,[46] we adapt it to the estimation of the absolute entropy of water within the solvation shell, and the results of our calculations are included in Table 2a, too. It should be noted, however, that using this method also seems to be controversial. For the water molecules within the solvation layer (near the peptide surface) their environment is anisotropic, and therefore the results of the entropy calculations using Henchman's method may not be fully correct. However, in spite of the doubts expressed above,

from the results included in Table 2a it follows that *the average local structure* of water within the solvation shell changes relatively little compared to the bulk one. This important conclusion is strongly suggested by two independent entropy estimations, and therefore we believe it is true. This conclusion will also be confirmed in the next part of the text.

Exploiting the concept of decomposition of the $s^{(2)}_{WW}(r)$ quantity into three terms, it is possible to get a deeper insight into the structure of water using some integrated measure of its structural ordering. Recently, Esposito et al.,[41] following the idea first described by Debenedetti et al.,[40,47] have proposed to use two rational, entropy-based parameters for a description of the thermodynamic state of the system. These parameters are the translational order parameter, represented by the $s^{(2)}_{WW,trans}$ quantity, and the orientational one, represented in our notation by the sum $s^{(2)}_{WW,conf} + s^{(2)}_{WW,orient}$. Now, we adapt this idea to our systems using the quantities

$$s_{tra}(r) = \frac{s^{(2)}_{WW,trans}(r)}{N_W}$$
$$s_{con}(r) = \frac{s^{(2)}_{WW,conf}(r)}{N_W} \quad (29)$$
$$s_{ort}(r) = \frac{s^{(2)}_{WW,conf}(r) + s^{(2)}_{WW,orient}(r)}{N_W}$$

calculated at two distances: $r = 0.36$ nm and $r = 0.58$ nm. These quantities represent the translational, configurational, and total orientational contribution to the local ordering, respectively, recalculated per one water molecule. The results are presented in Table 2b, and also (at $r = 0.58$ nm) graphically in Figure 2a, in the form of an "ordering map". This map represents, in a synthetic way, structural changes in water within the solvation layer; the point representing pure water properties is included in this graph, too. It is worthwhile to notice an interesting correlation: all the points representing the properties of "solvation" water lie approximately on a straight line. Moreover, comparing positions of particular points in Figure 2a, one can state that the investigated set of secondary structures of the polypeptide chain roughly divides into two subsets: the one containing a linear form, and the second one, which includes three helices: PII, $3_{10}$, and α. Note that this division is clearly visible for both peptides. We will return to this observation in subsection e, and also in further discussion presented in the Concluding Remarks.

Investigating the properties of pure water shows an almost strictly linear correlation between $s^{(2)}_{WW,conf}$ and $s^{(2)}_{WW,orient}$.[39] Unfortunately, for water within the solvation shell this simple correlation does not work, although we observe a similar general tendency. Nevertheless, as can be deduced from both Figure 2b and numerical data included in Table 2b, we still can use the $s_{con}(r)$ quantity instead of $s_{ort}(r)$ one. So, we propose to use the $s^{(2)}_{WW,conf}$ value as an approximate (qualitative only) measure of orientational ordering instead of the $s^{(2)}_{WW,conf} + s^{(2)}_{WW,orient}$ quantity. The main advantage of such a measure is that $s^{(2)}_{WW,orient}$ can be determined with relative ease, unlike $s^{(2)}_{WW,orient}$. Its obvious disadvantage, however, is only a poor correlation with the correct measure of $s^{(2)}_{WW,conf} + s^{(2)}_{WW,orient}$.

(c) Now, we use another way to study the structural properties of "solvation" water. An important factor that determines structural ordering in liquid water is, of course, the hydrogen bond network. Thus, we take into account both the geometry

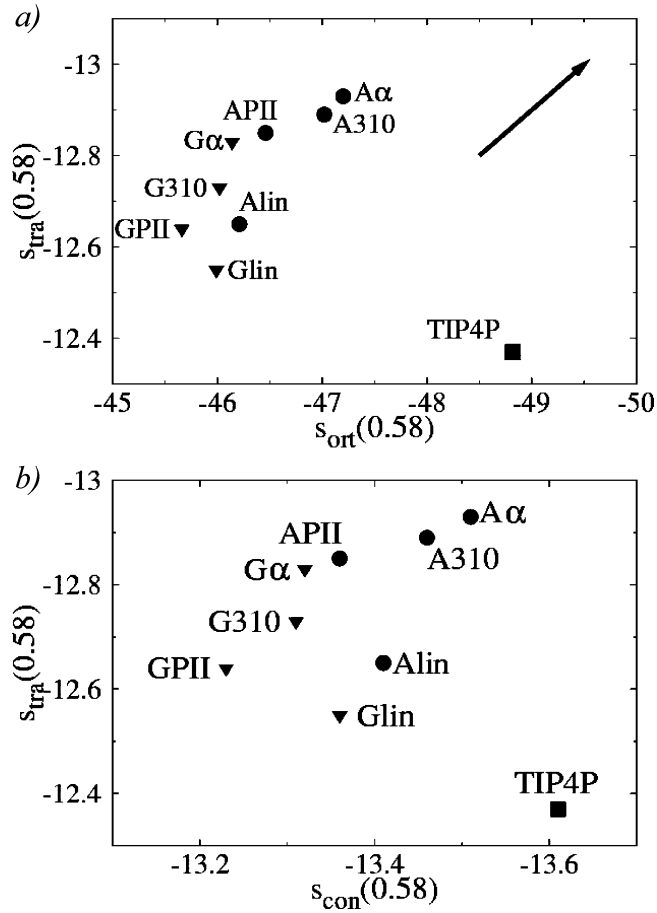


**Figure 2.** Ordering map. Plots of relations: (a) $s_{tra}(0.58) = f(s_{ort}(0.58))$ and (b) $s_{tra}(0.58) = f(s_{con}(0.58))$ (see text). Circles represent polyalanine, triangles describe polyglycine, and square represents pure water. The bold arrow in Figure 2a represents the direction of increasing ordering of the water structure.

of the water−water hydrogen bond network and the mean geometry of a single such bond.

To describe the hydrogen bond network structure, we slightly modified Chau and Hardwick's[42] idea. To describe the local water ordering, these authors introduced the well-known "tetrahedral ordering parameter": after selection of four nearest oxygen atoms that surround a tagged "central" water molecule, they calculate six angles between the vectors that link the selected atoms with the central water molecule oxygen atom. In our work this idea is modified as follows. Investigating a single snapshot of the trajectory file, we take into account, for a tagged "central" water molecule, all the partners bonded (by the hydrogen bond) with this molecule; the number of such partners, of course, is not fixed. Next, we calculate, similarly the proposal by Chau and Hardwick, all the angles between the vectors linking the oxygen atom of the central water molecule with the oxygen atoms of all its partners. Adopting this procedure to all water molecules, and repeating it over the whole trajectory file, we build a histogram describing the probability distribution for such angles. The obtained histogram has been normalized, assuming a total area bounded by the graph equals to 100. This histogram reflects the (geometrical) structure of the hydrogen bond network.

The results of such calculations are presented in Figure 3 as the differences between the histogram values calculated for "solvation" water, $P_{sol}$, and the ones calculated for bulk water, $P_{bulk}$; for comparison, we also include (in inset) the histogram values, $P_{bulk}$, calculated for bulk water. Note that this histogram

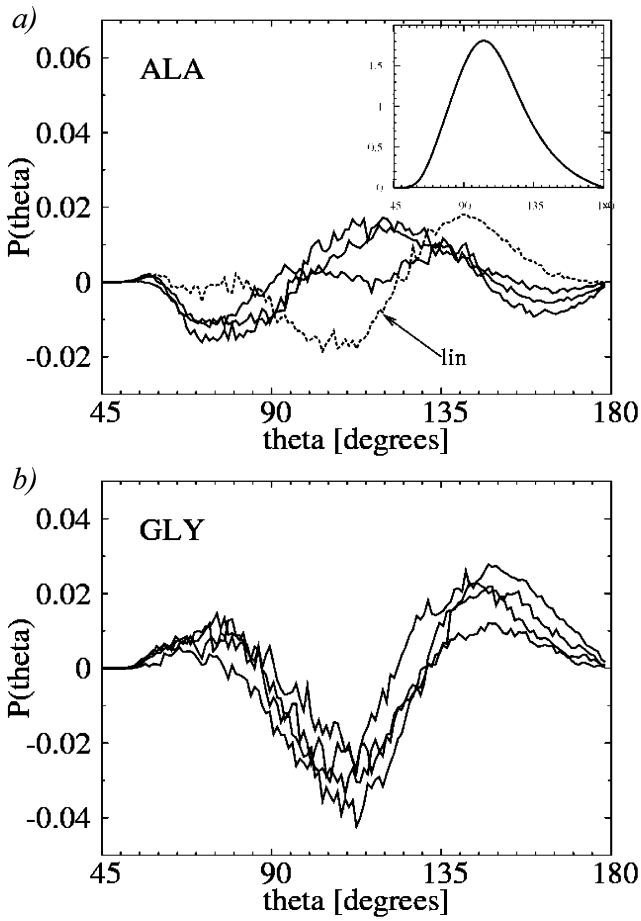


**Figure 3.** Presentation of the differences ($P_{solv} - P_{bulk}$) between the probability distribution of "tetrahedral" angles (see text) within solvation layer, $P_{solv}$, and the one in the bulk water, $P_{bulk}$. In the inset we include (for comparison purposes) the histogram for bulk water. For more clarity, the graph describing linear form of polyalanine is plotted using a dotted line.

confirms roughly tetrahedral structure of the hydrogen bond network in pure water, as it was reported previously (see Figure 3 in ref 39) with the angle between adjacent bonds equal to 109° approximately.

Two important deductions can be outlined from these results. First, the most visible fact is that the angle distribution for hydration water remains nearly unaltered in comparison to bulk water. The small differences do not exceed a few percent. It confirms our previous conclusion that structure of "solvation" water differs only slightly from the bulk one. In other words, the geometry of the water−water hydrogen bond network within the solvation layer is similar to the geometry of the bulk one. However, the word "similar" does not mean "the same": in fact, we observe some systematic deviations on the graphs representing the differences between the calculated probability distributions for water within solvation layer, $P_{solv}$, and the ones calculated for bulk water, $P_{bulk}$. Second, significant differences between the alanine- and the glycine-based peptides are visible: the alanine-based peptides disturb the hydrogen bond network in a smaller range, and in different way than the glycine ones. As may be seen, for water around three polyalanine helices the histogram indicates an increasing ordering: the tetrahedral angle (∼109°) is slightly more probable, while around the polyglycine conformations it is slightly less probable. It is very interesting to note, however, that the linear form of the alanine peptide behaves similarly to the glycine ones. This fact corresponds with the position of the point representing this form on the ordering map, as described in the previous subsection. We return to these remarks in subsection e, and also in the Concluding Remarks.

To analyze the properties of a single hydrogen bond, we take into account the mean number of hydrogen bonds per water molecule, the mean energy of this bond, and the probability distributions of the following quantities (see eq 1): the $\beta_{OOH}$ angle, the oxygen−oxygen distance, $R_{OO}$, and the hydrogen-bond length $d_{OH}$. All these properties have been determined within the first and second solvation layers separately (and also, needless to say, for pure water). The results are collected in Table 3, along with the properties of bulk water. The most visible result is an increase in the mean energy of the hydrogen bond within the first solvation shell, by 0.2−0.3 kJ/mol, approximately. The same behavior was also reported previously for the polyglycine.[23] Moreover, the mean geometry of a single hydrogen bond, observed within the first solvation layer, changes only slightly in comparison to the one in bulk water. To obtain more detailed description, we inquired how the probability distributions (of $\beta_{OOH}$, $R_{OO}$, and $d_{OH}$) within the solvation layer deviate from the ones for bulk water. Figure 4 shows the difference of such probability distributions between "solvation" water and the bulk one, presented for two quantities: the angle $\beta_{OOH}$, and the oxygen−oxygen distance, $R_{OO}$. In general, the observed differences are very small, confirming our previous conclusion about small structural changes within "solvation" water. It may be seen that for the alanine polypeptide the observed changes are considerably less distinct than for the glycine one. Some differences between various conformations of the peptide chain are observed, and as can be seen, these differences correspond to the results and conclusions we express in subsection b.

Finally, we can say that all the results presented here still agree with the previously deduced conclusion: the structure of "solvation" water changes only slightly in comparison to the one in bulk water. Nevertheless, comparing both the alanine- and the glycine-based polypeptides, we conclude that they disturb the water structure by another way.

(d) The aim of this work is investigation of the structural properties of water around the peptide core. However, it seems to be quite obvious that any changes in water structure around the peptide core will have an influence on many physical properties of such "solvation" water. Therefore, we also wish to take into account some dynamic quantities, such as the self-diffusion coefficients (including the translational and rotational ones) and the mean lifetime of a single water−water hydrogen bond. We expect these results to confirm our deductions obtained so far and also, maybe, allow us to gain a deeper insight into the structure of "solvation" water.

The results of measurements of both the diffusion coefficients and the lifetimes are included in Table 4. Because the hydrogen bond decays nonexponentially[48,49] as a function of time $t$, we use the two-exponential relation:

$$S_A(t) = A_T e^{-t/\tau_T} + A_R e^{-t/\tau_R} \tag{30}$$

for description of the obtained $S_A(t)$ data.[23] Thus, in Table 4 we present two values, $\tau_R$ and $\tau_T$, along with the respective $A_R$ and $A_T$ ones (all the parameters were adjusted using the least-squares method).

A glance at this table shows that water molecules within the solvation shell move slowly; the value of the translational diffusion coefficient, $D_T$, within the first solvation shell is

**TABLE 3: Structural Properties of the Water−Water Hydrogen Bonds within the First (I) and the Second (II) Solvation Shell around Various Structural Forms of the Polyalanine[a]**

| | $n_{HB}$ | | $E_{HB}$ [kJ/mol] | | $R_{OO}$ [nm] | | $\beta_{OOH}$ [deg] | |
|---|---|---|---|---|---|---|---|---|
| conformation | I | II | I | II | I | II | I | II |
| Alin | 3.02 | 3.20 | 17.62 | 17.48 | 0.2818 | 0.2818 | 12.74 | 12.84 |
| APII | 3.02 | 3.21 | 17.65 | 17.50 | 0.2817 | 0.2818 | 12.66 | 12.81 |
| A310 | 3.05 | 3.21 | 17.73 | 17.48 | 0.2818 | 0.2819 | 12.66 | 12.82 |
| Aα | 3.05 | 3.21 | 17.82 | 17.48 | 0.2818 | 0.2818 | 12.59 | 12.81 |
| estimated error limits | ±0.03 | ±0.01 | ±0.03 | ±0.02 | ±0.0001 | ±0.0001 | ±0.05 | ±0.05 |
| bulk water | 3.21 ± 0.01 | | 17.50 ± 0.01 | | 0.2819 ± 0.0001 | | 12.82 ± 0.01 | |

[a] $n_{HB}$, $E_{HB}$, $R_{OO}$, and $\beta_{OOH}$ represent the mean number of hydrogen bonds per water molecule, the mean energy of this bond, the mean distance oxygen−oxygen, and the O−O−H angle, respectively.

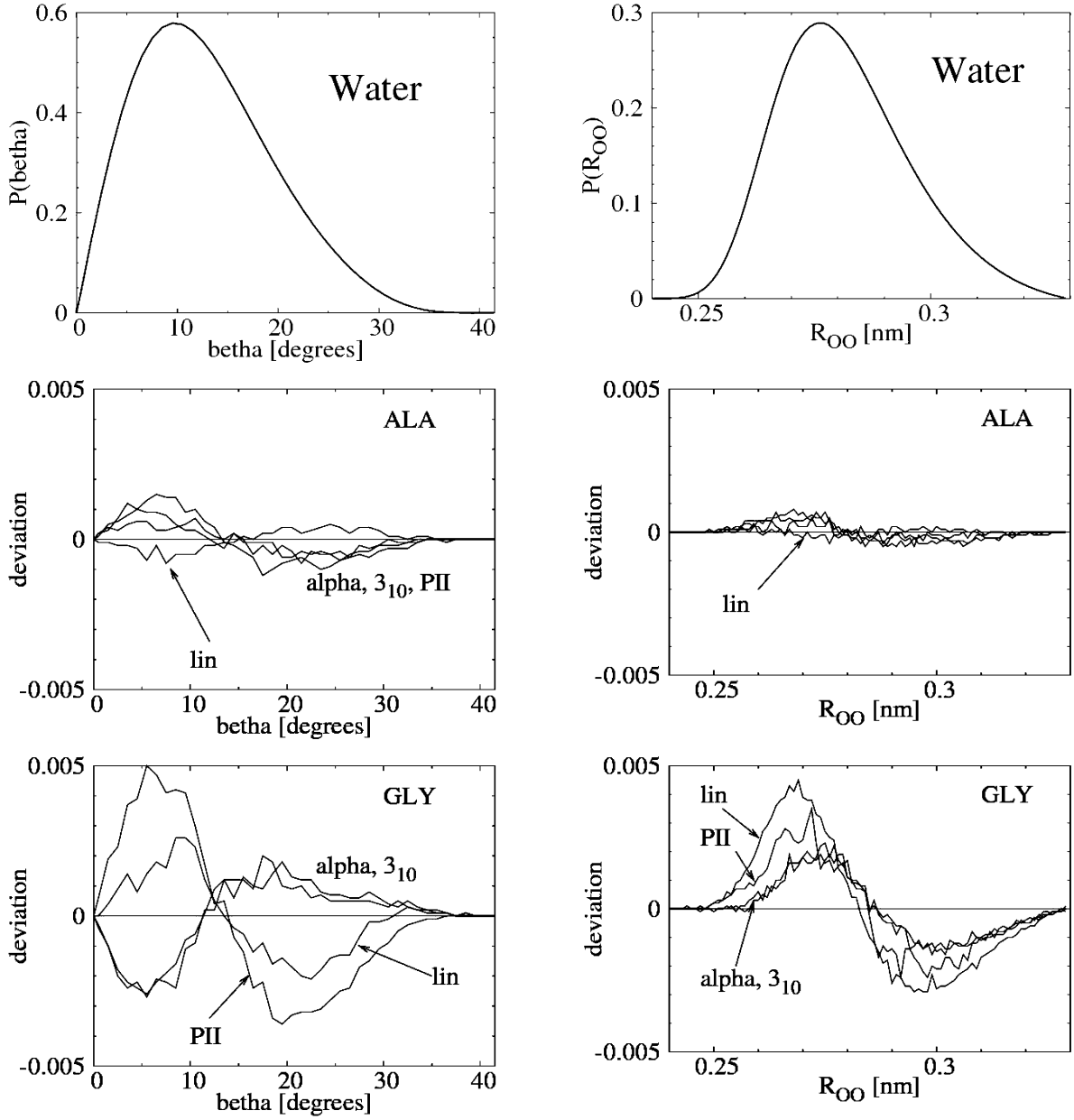


**Figure 4.** The differences ($P_{solv} - P_{bulk}$) in probability distributions of the hydrogen bond angle, $\beta_{OOH}$, and the oxygen−oxygen distance, $R_{OO}$, between first solvation shell and the bulk one. Left column shows deviation (from bulk water properties) of $\beta_{OOH}$ distribution, while the right one describes deviation of the oxygen−oxygen distance.

significantly smaller (up to 50% approximately) than the one for bulk water. It is interesting to note, however, that rotational diffusion (described by the $D_R$ coefficient) within the first solvation layer also decreases, but in a significantly lower range (15−20% approximately). We also observe augmentation on both the $\tau_R$ and $\tau_T$ values for "solvation" water compared to those for the bulk one. The decrease in diffusion coefficient is a well-known result, and it has been observed for many systems.[1,12] Note that slowing down of both rotational and translational motions is more clearly visible for polyalanine than

**TABLE 4: Dynamic Properties of Water within the First (I), and the Second (II) Solvation Shell around Various Structural Forms of the Polyalanine[a]**

| | $10^9 D_T$ [m$^2$/s] | | $10^{-11} D_R$ [rad$^2$/s] | | $A_Y$ | | $A_R$ | | $\tau_T$ [ps] | | $\tau_R$ [ps] | |
|---|---|---|---|---|---|---|---|---|---|---|---|---|
| conformation | I | II | I | II | I | II | I | II | I | II | I | II |
| Alin | 2.12 | 3.25 | 2.45 | 2.91 | 0.74 | 0.75 | 0.25 | 0.24 | 0.50 | 0.46 | 0.11 | 0.11 |
| APII | 2.07 | 3.30 | 2.42 | 2.97 | 0.72 | 0.74 | 0.27 | 0.25 | 0.48 | 0.41 | 0.11 | 0.10 |
| A310 | 2.17 | 3.38 | 2.43 | 3.02 | 0.76 | 0.75 | 0.24 | 0.25 | 0.50 | 0.45 | 0.12 | 0.11 |
| Aα | 1.95 | 3.35 | 2.39 | 2.81 | 0.74 | 0.76 | 0.25 | 0.24 | 0.50 | 0.44 | 0.12 | 0.10 |
| estimated error | ±0.1 | ±0.1 | ±0.2 | ±0.2 | ±0.05 | ±0.03 | ±0.05 | ±0.02 | ±0.02 | ±0.01 | ±0.02 | ±0.01 |
| bulk water | 3.76 ± 0.1 | | 3.06 ± 0.1 | | 0.77 ± 0.01 | | 0.23 ± 0.01 | | 0.43 ± 0.01 | | 0.10 ± 0.01 | |

[a] $D_T$ and $D_R$ represent the translational and the rotational diffusion coefficients, respectively. $A_i$ and $\tau_i$ denote parameters in the biexponential fit of the $S_A(t)$ function (eq 30).

for polyglycine (see ref 23 for comparison of the results). It may be caused by the presence of the side groups ($CH_3$),[50] and this effect will be considered in more detail in subsection e. For the second solvation layer, however, both diffusion coefficients, $D_T$ and $D_R$, differ from the bulk value by a few percent only. As in our previous paper,[23] we link this behavior (the slowing down both translational and rotational moves) with the two time constants in eq 30, $\tau_T$ and $\tau_R$, which describe the decay of the hydrogen bonds (between water molecules) in time. According to this idea, we assume that a hydrogen bond may break in two general ways: by stretching or by bending itself. Both these breaking mechanisms (stretching and bending) are governed by the translational and rotational diffusion, respectively, and therefore, their relaxation times differ. So, the enlarging $\tau_T$ value conforms to the appropriate change in the translational diffusion coefficient, $D_T$. On the other hand, the $\tau_R$ value changes slightly, and this corresponds to the slightly changing $D_R$ coefficient.

This concept, however, seems to be in contrast to the well-founded model recently proposed by Laage and Hynes.[51,52] Within this model, the large amplitude (68° approximately[52]) angular jumps are assumed to be responsible for the reorientation of water molecule, and therefore for the hydrogen bond exchange. In other words, the hydrogen bond breaking−forming mechanism is fundamentally the nondiffusive one. Thus, we wish now to reconcile the observed correlation between two time constants and two diffusion coefficients with the Laage and Hynes' "jumping" model. Our argument is as follows (for more clarity we use the same symbols as in ref 52).

We assume that a water O*H* is initially H-bonded to a water oxygen $O^a$ (the acceptor of proton H*) and, after breaking this bond, it becomes H-bonded to a new water oxygen, $O^b$. Two obvious conditions should be fulfilled for a successive jump, and therefore for hydrogen bond exchange: (1) the water oxygen $O^b$ must be present in an appropriate space region within the second hydration shell around the oxygen $O^a$, and (2) the orientation of the water molecule $H_2O^b$ (toward the oxygen $O^a$) should also be appropriate. However, the nature of molecular motions of water within this shell−at the distance 0.43 nm or more (see Figure 3 in ref 52)−is the diffusive one. This is why the above-described correlation between both the diffusion coefficients, $D_T$ and $D_R$, and the two time constants, $\tau_T$ and $\tau_R$, is observed.

If our reasoning is true, the following conclusions can be outlined from it. At first we note that the orientational (rotational) fitting, by diffusive motions, of the water $O^b$ oxygen is a much faster process than looking for an appropriate (close enough) position within the hydration shell. Therefore, the rotational time constant, $\tau_R$, should be clearly shorter than the translational one, $\tau_T$. Moreover, since translational diffusion of the water molecule, $H_2O^b$, within the second hydration layer is the main factor that limits the process of H-bond exchange, the coefficient $A_T$ (which measures participation of translation in this process) should be clearly greater than $A_R$, and this is what we have observed. Another prediction concerns the temperature dependence of the $A_i$ and $\tau_i$ coefficients. Because the diffusion coefficients $D_T$ and $D_R$ roughly fulfill the Arrhenius temperature dependence (with the same activation energy, equal to 12.7 kJ/mol approximately,[53] determined within the 278−363 K temperature range), we expect that ratios $\tau_T/\tau_R$ and $A_T/A_R$ should be temperature independent, and just such effects have been observed.[53]

The values of $A_i$ (given in Table 4 too) measure the participation of both the above-mentioned mechanisms in the hydrogen bond breaking (exchange) process. Keeping in the mind the above considerations, we should pay attention to slight changes in the $A_i$ values within the first solvation shell as compared to the ones in bulk water. Two effects may be responsible for such changes. First, the influence of the hydrophobic effect on elongation of the hydrogen bond lifetime; this effect was investigated in detail by Laage and Hynes.[54] Second, the hydrophilic interactions (as hydrogen bonding) between water and the selected peptide atoms (the amide group and the oxygen). Both of these effects may lead to some modification of the hydrogen bond breaking mechanism, and it is our suggestion that observed changes in $A_i$ values reflect such alteration. This suggestion can also be supported by some recent literature reports. Jana et al.[55] have considered the "jumping" mechanism within the solvation layer of lysozyme. They found that within this layer only 80% of hydrogen bond breaking events proceed under the same mechanism as in bulk water. Unfortunately, it is difficult to deduce more details about it from our results.

The enlargement of both time constants, $\tau_T$ and $\tau_R$, within the first solvation shell (relative to the one for bulk water) corresponds to an appropriate rise in the hydrogen bond energy (see Table 3). In our opinion, however, a primary reason of all observed phenomena are the orientational effects, forced by the presence of the peptide core. They lead, as a result, to a hydrogen bond energy increase, and therefore to a hindered translation of water molecules. Moreover, the hindered translation is also the result of the existence of the peptide molecule, as the "hard wall" effect. The hindered rotation, however, is only a result of the higher energy of the hydrogen bond. Since this energy is increased insignificantly, the rotational diffusion also decreases only slightly. In other words, from the above argument it arises that the rotational diffusion coefficient, $D_R$, can serve as the more appropriate dynamic measure of the local structural changes than $D_T$. A similar opinion has also been expressed by Halle.[56] Therefore, the presented analysis of the dynamic properties of water within the solvation layer also supports our previously expressed statement that the structure

of such "solvation" water changes only slightly in comparison to the bulk one, in spite of significant changes in values of the translational diffusion coefficient, $D_T$.

(e) The above deliberations suggest that the structure of water within the solvation layer should be a bit more rigid than the structure of bulk water, because of the slightly higher mean energy of a single water−water hydrogen bond. This suggestion can be also confirmed by a spectral analysis of water molecules motion.

As reported in the literature, the power spectrum of velocity (calculated from the velocity autocorrelation function) covers two main regions: 0−250 and 200−800 $cm^{-1}$, and these regions correspond to the translational and the rotational vibrations of the water molecule,[57,58] respectively. The power spectra calculated in this work are very similar to the ones for polyglycine, showing a characteristic displacement of the main peak in the translational part of the power spectrum toward higher frequencies, by $\sim$10 $cm^{-1}$ approximately. Our argument is also similar, and therefore we are only repeating the final conclusion expressed earlier:[23] the structure of water in the vicinity of the peptide core is more rigid than the structure of bulk water. It should be noted here that such a conclusion seems to be trivial to some extent, because not only do we not observe any significant differences between both the glycine- and alanine-based peptides but also a very similar shift ($\sim$10 $cm^{-1}$) of the main peak in the power spectrum was observed previously in various systems.[22,57,58] Thus, the increasing rigidity of water within the hydration layer is a rather general property, which arises as a consequence of the orientational effects of water molecules within the hydration layer, as discussed in previous subsection d.

The results hitherto presented allow us to presume that water molecules form some cohesive structure around the peptide core, and this "halo" is stabilized by the presence of this core as well as by the hydrogen bond network. In our previous paper[23] it was found (for glycine-based peptides) that this "halo" is not closely connected with the solute core. For alanine, however, we expect another behavior.

To examine this expectation, at the start we have calculated the radial distribution functions of the water molecule's oxygen and hydrogen atoms around the peptide carbonyl oxygen, nitrogen, and (amide) hydrogen. These results indicate the existence of specific interactions (hydrogen bonding), especially between the peptide oxygen and water. We have also observed interactions between the amide hydrogen and water, but they are relatively weak compared to the ones between the carbonyl group oxygen and water. In the case of the linear form of peptide, the obtained radial distribution functions confirm the presence of water bridges, previously noticed by Mezei et al.[59] in the polyalanine $\beta$-strands. This fact also explains, in our opinion, why the linear form clearly deviates from the other ones in both Figures 2 and 3, as reported in subsections b and c.

Next, we calculate the "residence time" of the water hydrogen around the carbonyl oxygen; this quantity has been calculated as follows. At the beginning we presuppose that the mentioned hydrogen bond exists if the interatomic distance between the peptide oxygen and the water hydrogen, $d_{OH}$, does not exceed 0.25 nm (this is the position of minimum on the $g_{OH}(r)$ function). Then, using the time correlation function $S_A(t)$ defined by eq 4, we calculate the mean lifetime of a so-defined bond, and we call it "residence time". Similarly to the water−water hydrogen bonds, and for the same reasons, eq 30 correctly fits the $S_A(t)$ function. We also accept the same interpretation of both time constants: the quantity $\tau_T$ reflects the translational mechanism of the hydrogen bond exchange process, while the quantity $\tau_R$ can be linked with the rotational one.

**TABLE 5: Parameters of the Function Describing the Residence Time of the Water Hydrogen around the Carbonyl Oxygen of Peptide, for Various Conformations of the Polypeptide Molecule[a]**

| conformation | $\tau_T$ [ps] | $\tau_R$ [ps] |
|---|---|---|
| Alin | 2.35 ± 0.10 | 0.49 ± 0.10 |
| APII | 3.00 ± 0.10 | 0.66 ± 0.10 |
| A310 | 2.49 ± 0.10 | 0.47 ± 0.10 |
| Aα | 2.49 ± 0.10 | 0.56 ± 0.10 |
| Glin | 1.44 ± 0.05 | 0.27 ± 0.05 |
| GPII | 1.78 ± 0.05 | 0.41 ± 0.05 |
| G310 | 1.64 ± 0.05 | 0.27 ± 0.05 |
| Gα | 1.50 ± 0.05 | 0.29 ± 0.05 |
| water TIP4P[b] | 2.36 ± 0.02[b] | 0.51 ± 0.02[b] |

[a] $\tau_T$ and $\tau_R$ denote two time constants in bi-exponential fit of $S_A(t)$ function (eq 30). [b] The values for pure TIP4P water cited in this table were calculated using the "distance only" criterion in place of the Wernet et al.[25] definition, using $d = 0.25$ nm as the limiting value of the hydrogen−oxygen distance.

The results are included in Table 5. This table also contains, for comparison purposes, the results obtained for the glycine polypeptide. As for the calculations of the two-particle contribution to entropy, we do not use previous results, but we repeat calculations for the glycine-based peptide using the same force field (Amber ff03) and the same water model (TIP4P) as for polyalanine. Moreover, for comparison of these results with the mean lifetime of the water−water hydrogen bond, we also determine the lifetime of this bond by using the "distance only" criterion in place of the previously used Wernet et al.[25] definition and by using $d = 0.25$ nm as the limiting value for the hydrogen−oxygen distance.

Significant differences between the glycine- and alanine-based peptides are observed. The most visible fact is the clear enlarging (roughly twice) of both $\tau_T$ and $\tau_R$ values for polyalanine compared to the ones for polyglycine. Moreover, the "residence times" determined for the glycine-based polypeptides are roughly half the values for a single hydrogen bond between two water molecules, calculated using the same "distance only" criterion (see the last row in Table 5). We conclude, therefore, that in the case of glycine the solvation layer is not tightly connected with the peptide core, and it can slide (relatively easily) on the peptide surface. For the alanine peptides, however, the time constant $\tau_T$ is enlarged, which means that this "sliding" is strongly hindered, because of the presence of the methyl groups. Because the sliding of the water layer on the peptide surface causes rotation of the water molecules bonded to the peptide oxygen, its rotation is hindered too. As a result, the time constant $\tau_R$ also is clearly enlarged. In other words, the above-mentioned "halo" of water molecules is additionally immobilized near the alanine peptide surface by the side groups, and the elongation of both $\tau_T$ and $\tau_R$ time constants included in Table 5 (compared to the values for glycine), can serve as a measure of this effect. Thus, analysis of the "residence times" allows us to perceive and to explain distinct differences in dynamics of the solvation shell around both glycine and alanine peptides.

## Concluding Remarks

This work continues systematic investigations of the solvation shell properties around various structural forms of simple polypeptides. A primary purpose of this article was to describe

structural properties of water within the solvation shell, and also to link them with various physical properties of water within the solvation layer. The main results of this work can be summarized as follows.

First, we propose using the two-particle contribution to entropy for describing structural ordering of water within the solvation layer. As can be read from eq 9, this contribution divides into three terms, depending on the peptide−peptide, peptide−water, and water−water interactions, respectively. The term depending on the peptide−water interactions describes an arrangement of water molecules around the peptide core, while the structure of the "solvation" water is described by the term depending on the water−water interactions. In this work we take into account both these terms, and this is the first such attempt.

Analysis of the term depending on the peptide−water interactions leads to the conclusion that water molecules show marked orientations relative to the peptide surface. The values of the $s^{(2)}_{PW}$ term are generally similar for both the alanine and glycine, and the differences between both peptides reflect the presence of hydrophobic $CH_3$ group in alanine.

The term depending on the water−water interactions seems to be much more interesting; unfortunately, its estimation is a very hard task. Although the two-particle approximation leads to reliable results if it is adapted to the description of pure water properties,[38,39,41] its utility for the description of water in the nearest neighborhood of the peptide molecule requires some other approximations. Under such approximations, and exploiting our previously published results,[38,39] we propose a rational measure of water's local structural ordering within the solvation shell. We have also shown that this measure can be divided into three terms describing the translational, configurational, and orientational contributions to the local ordering.

Because of the mentioned approximations, we also employ an independent (harmonic approximation) method for an estimation of the entropy. Both these methods lead to the same weighty conclusion that the local structure of such "solvation" water changes only slightly compared to that of the bulk water. Also further investigations of various properties, such as the structure and the dynamics of the water−water hydrogen bonds, the diffusion coefficients, and the analysis of the hydrogen bond lifetimes confirm this conclusion.

Exploiting the introduced measure of local structural ordering, and following the idea presented by other authors,[41] we use two parameters: $s_{tra}$ and $s_{ort}$ (see eq 29) for building the ordering map, which more precisely describes the local ordering of water within the solvation layer. As has been found, the position of the point representing "solvation" water on this map differs from the one for bulk water, and these differences depend on the secondary peptide structure. Thus, such a map gives both qualitative and quantitative description of water's structural changes within this region. An interesting correlation has been observed: the points on this map, representing various helical peptide structures, lie approximately on a straight line, while the linear conformation clearly deviates from the general tendency. Note that our measure allows us to distinguish the properties of "solvation" water around various secondary structures of the peptide chain, and it is not a trivial result.

Very interesting deductions may also be outlined from the positions of points in this ordering map. The bold arrow in Figure 2a represents the direction of increasing ordering of the water structure (see a discussion concerning eqs 16−18 in the Method section; this argument is also true, of course, for the $s_{tra}$, $s_{con}$, and $s_{ort}$ quantities). Thus, it can be stated that the local water structure is more ordered around alanine-based peptides than in the vicinity of the glycine ones. This important observation, first noted in subsection c, is worthy of special attention, and it also deserves some deeper analysis presented below.

It is well-known that alanine is a much better "helix former" than glycine.[5] To describe this tendency in terms of quantity, López-Llano et al.[60] have investigated an influence of various physical reasons for the stabilization of the α-helix created by both alanine- and glycine-based polypeptides. They have found that the backbone entropy difference contributes only 15% to total stabilization of the α-helix by the alanine polypeptide relative to the glycine one. A large part (35%) originates from the increased hydrophobic effect of alanine compared to glycine, while the remaining 50% originates from the sum of enthalpic effects. In other words, the impact of solvation effects is very large, even predominant. On the other hand, comparing (on our ordering map) the position of points representing the α-helical structure created by both alanine- and glycine-based polypeptides, it is easy to see that increasing local ordering of water corresponds with increasing stability of both these helices. Therefore, it is conceivable that the measure of local structural ordering introduced by us (which, after all, reflects, in some way, the structure of surrounding water) is correlated with the stability of particular structures in water solution. To test this conjecture, we should know, even approximately, the values of the stability constants. Unfortunately, their numerical values are unavailable, and therefore we want now to make such an evaluation. Our argument is as follows.

Many literature reports[61−65] indicate that in water solution the polyalanine PII helix is preferred in comparison with the extended $\beta$ structure. Moreover, it has been shown[63,64] that water is the least disturbed by the PII helix as compared to the linear form; note that a similar conclusion has also been derived in our previous paper[23] for polyglycine. It is caused by the presence of the above-mentioned "water bridges", reported by Mezei et al.,[59] while more solvent-exposed structure of PII helix facilitates its "building in" to the existing structure of surrounding water. This explains why the PII structure is preferred.[64] Because in our ordering map the position of the points representing the linear conformation for both peptides indicates the smallest local ordering of the water structure around this form than the ordering around the PII one, comparison of both linear and PII structures confirms our above expressed supposition.

It seems that comparison of the α-helix with the $3_{10}$ helix (both created by polyalanine) leads to the same conclusion: Yang and Cho,[66] investigating thermal denaturation of polyalanine α-helix, have found significant contents of $3_{10}$ helix for all the investigated temperatures. Similarly, Young and Brooks[67] have shown that the $3_{10}$ helix plays a role in helix formation. Therefore, it is rational to suppose that the $3_{10}$ helix is a bit less stable in water solution than the α-helix.

Unfortunately, for the glycine-based peptides, the argument presented above fails, because, as shown recently by Tran et al.,[68] in water solution polyglycine forms compact, albeit disordered, globules. Therefore, excluding the above-mentioned comparison of both linear and PII forms of polyglycine, it is difficult to judge the relative stability of a particular secondary structure of this peptide.

Our above-presented presumption that local structural ordering correlates with the stability of a particular structure in water solution may be also supported by another observation. As mentioned in subsection c, the linear form of polyalanine disturbs the hydrogen bond network in a way similar to that

for all the polyglycine structures (see Figure 3), but in a different way from that of the remaining (and more stable) polyalanine conformations: PII, $3_{10}$ helix, and α-helix. Moreover, for water around the three polyalanine helices the histogram suggests a higher ordering: the tetrahedral angle (∼109°) is slightly more probable, while around the polyglycine conformations it is slightly less probable. Therefore, Figure 3 also supports our supposition, but in a less precise (only qualitative) manner.

Accepting usefulness of the introduced measure of local structural ordering, we put forward using the $s_{con}$ quantity (defined by eq 29) instead of the $s_{ort}$ one as an approximate measure of the orientational contribution to the local structural ordering of "solvation" water. Using this quantity, along with the $s_{tra}$ one, we also can build the ordering map. The picture obtained in this case is very similar, in terms of quality, to the one obtained by using the $s_{tra}$ and $s_{ort}$ variables. Therefore, the $s_{con}$ quantity can serve as a solely approximate, but compact and easy to determine, measure of the structural ordering of water within the solvation layer around the peptide core. In our opinion, this parameter may be used as a rational alternative to the well-known empirical tetrahedral ordering parameter, previously proposed in the literature.[42]

Some interesting deductions about the properties of "solvation" water may be also outlined from the analysis of dynamic properties. From the detailed survey of the velocity autocorrelation functions it follows that water within the solvation layer creates a pseudorigid structure. Combining this fact and the remaining results, we can say that water surrounding the peptide core forms a "halo" around it. This "halo" is stabilized by slightly higher energy of the hydrogen bonds network: we have found that (within this "halo" region) the hydrogen bonds are slightly less distorted, they are somewhat more stable and their mean lifetime is longer compared to that of bulk water. Note that significant differences between the alanine- and glycine-based peptides are observed. Moreover, some of our results suggest that the hydrogen bond dynamics in the vicinity of the polyalanine core may differ from the one in bulk water, and we suppose that this difference may be brought about by modification of the "jumping" mechanism of the hydrogen bond exchange process.

Next, investigating the "residence times" of water near the peptide surface it has been discovered that the solvation layer interacts with the peptide surface in two ways. First, it creates the hydrogen bonds, mainly in the carbonyl group oxygen atoms, but the ones created with the amide group hydrogen atom are also present (it is especially visible for the linear conformation). Second, it interacts with the bulky side groups ($CH_3$) of polyalanine: in the case of the glycine-based polypeptides the layer slides relatively freely over peptide surface, while for the alanine-based polypeptides this sliding is strongly hindered by the presence of the methyl groups; this effect is additionally enhanced by the rise in the solvation layer rigidity. So, such analysis allows us to perceive and to explain distinct differences in behavior of water within the solvation shell around both the glycine and alanine peptides.

**Acknowledgment.** We thank the reviewers for their valuable comments. The calculations were carried out at the Academic Computer Center (TASK) in Gdańsk. This work was also partially supported by the Republic of Poland within the research grant No. N N204 3799 33.

**Supporting Information Available:** Table of dynamic properties of pure TIP4P water as a function of temperature. Arrhenius plots. This material is available free of charge via the Internet at http://pubs.acs.org.

## References and Notes

(1) Prabhu, N.; Sharp, K. *Chem. Rev.* **2006**, *106*, 1616.
(2) Ball, P. *Chem. Rev.* **2008**, *108*, 74.
(3) Levy, Y.; Onuchic, J. N. *Annu. Rev. Biophys. Biomol. Struct.* **2006**, *35*, 389.
(4) Wang, C.; Liu, L.-P.; Deber, C. M. *Phys. Chem. Chem. Phys.* **1999**, *1*, 1539.
(5) Krittanai, C.; Johnson, W. C. *Proteins: Struct. Funct. Genet.* **2000**, *39*, 132.
(6) Kohtani, M.; Jones, T. C.; Schneider, J. E.; Jarrold, M. F. *J. Am. Chem. Soc.* **2004**, *126*, 7420.
(7) Sorin, E. J.; Rhee, Y. M.; Shirts, M. R.; Pande, V. S. *J. Mol. Biol.* **2006**, *356*, 248.
(8) Levy, Y.; Jortner, J.; Becker, O. M. *Proc. Natl. Acad. Sci. U.S.A.* **2001**, *98*, 2188.
(9) Nguyen, H. G.; Marchut, A. J.; Hall, C. K. *Protein Sci.* **2004**, *13*, 2909.
(10) Raschke, T. M. *Curr. Op. Str. Biol.* **2006**, *16*, 152.
(11) V. Helms, V. *ChemPhysChem* **2007**, *8*, 23.
(12) Bagchi, B. *Chem. Rev.* **2005**, *105*, 3197.
(13) Daggett, V. *Chem. Rev.* **2006**, *106*, 1898.
(14) Johnson, M. E.; Malardier-Jugroot, C.; Murarka, R. K.; Head-Gordon, T. *J. Phys. Chem. B* **2009**, *113*, 4082.
(15) Schlitter, J. *Chem. Phys. Lett.* **1993**, *215*, 617.
(16) Schäfer, H.; Mark, A. E.; van Gunsteren, W. F. J. *J. Chem. Phys.* **2000**, *113*, 7809.
(17) Andricioaei, I.; Karplus, M. *J. Chem. Phys.* **2001**, *115*, 6289.
(18) Harano, Y.; Kinoshita, M. *J. Chem. Phys.* **2006**, *125*, 024910.
(19) Harano, Y.; Kinoshita, M. *Biophys. J.* **2005**, *89*, 2701.
(20) Lin, S.-T.; Blanco, M.; Goddard, W. A. *J. Chem. Phys.* **2003**, *119*, 11792.
(21) Lin, S.-T.; Maiti, P. K.; Goddard, W. A. *J. Phys. Chem. B* **2005**, *109*, 8663.
(22) Jana, B.; Pal, S.; Maiti, P. K.; Lin, S.-T.; Hynes, J. T.; Bagchi, B. *J. Phys. Chem. B* **2006**, *110*, 19611.
(23) Kuffel, A.; Zielkiewicz, J. *J. Phys. Chem. B* **2008**, *112*, 15503.
(24) Case, D. A.; Darden, T. A. ; Cheatham, T. E., III; Simmerling, C. L.; Wang, J.; Duke, R. E.; Luo, R.; Crowley, M.; Walker, R. C.; Zhang, W.; Merz, K. M. ; Wang, B.; Hayik, S.; Roitberg, A.; Seabra, G. ; Kolossváry, I.; Wong, K. F.; Paesani, F.; Vanicek, J.; Wu, X.; Brozell, S. R.; Steinbrecher, T.; Gohlke, H.; Yang, L.; Tan, C.; Mongan, J.; Hornak, V.; Cui, G.; Mathews, D. H.; Seetin, M. G.; Sagui, C.; Babin, V. Kollman, P. A. *AMBER 10*; University of California: San Francisco, 2008.
(25) Wernet, Ph.; Nordlund, D.; Bergmann, U.; Cavalleri, M.; Odelius, M.; Ogasawara, H.; Näslund, L. A.; Hirsch, T. K.; Ojamäe, L.; Glatzel, P.; Pettersson, L. G. M.; Nilsson, A. *Science* **2004**, *304*, 995.
(26) Chandler, D. *Introduction to Modern Statistical Mechanics*; Oxford University Press: New York, 1987.
(27) Green, H. S. *The Molecular Theory of Fluids*; North-Holland: Amsterdam, 1952; Chapter *III*.
(28) Nettleton, N. E.; Green, M. S. *J. Chem. Phys.* **1958**, *29*, 1365.
(29) Raveché, H. J. *J. Chem. Phys.* **1971**, *55*, 2242.
(30) Baranyai, A.; Evans, D. J. *Phys. Rev. A* **1989**, *40*, 3817.
(31) Baranyai, A.; Evans, D. J. *Phys. Rev. A* **1990**, *42*, 849.
(32) Wallace, D. C. *J. Chem. Phys.* **1987**, *87*, 2282.
(33) Wallace, D. C. *Phys. Rev. A* **1989**, *39*, 4843.
(34) Lazaridis, T.; Paulaitis, M. E. *J. Phys. Chem.* **1992**, *96*, 3847.
(35) Lazaridis, T.; Paulaitis, M. E. *J. Phys. Chem.* **1992**, *97*, 5789.
(36) Laird, B. B.; Haymet, A. D. J. *J. Chem. Phys.* **1992**, *97*, 2153.
(37) Lazaridis, T.; Karplus, M. *J. Chem. Phys.* **1996**, *105*, 4294.
(38) Zielkiewicz, J. *J. Chem. Phys.* **2005**, *123*, 104501; *J. Chem. Phys.* **2006**, *124*, 109901.
(39) Zielkiewicz, J. *J. Phys. Chem. B* **2008**, *112*, 7810.
(40) Truskett, T. M.; Torquato, S.; Debenedetti, P. G. *Phys. Rev. E* **2000**, *62*, 993.
(41) Esposito, R.; Saija, F.; Saitta, A. M.; Giaquinta, P. V. *Phys. Rev. E* **2006**, *73*, 040502.
(42) Chau, P.-L.; Hardwick, A. J. *Mol. Phys.* **1998**, *93*, 511.
(43) Press, W. H.; Teukolsky, S. A.; Vetterling, W. T.; Flannery, B. P. *Numerical Recipes in Fortran 77. The Art of Scientific Computing*, 2nd ed.; Cambridge University Press: Cambridge, U.K., 2001.
(44) Henchman, R. H. *J. Chem. Phys.* **2003**, *119*, 400.
(45) Henchman, R. H. *J. Chem. Phys.* **2007**, *126*, 064504.
(46) Zielkiewicz, J. *J. Chem. Phys.* **2008**, *128*, 196101.
(47) Errington, J. R.; Debenedetti, P. G. *Nature* **2001**, *409*, 318.
(48) Luzar, A.; Chandler, D. *Nature* **1996**, *397*, 55.
(49) Luzar, A.; Chandler, D. *Phys. Rev. Lett.* **1996**, *76*, 928.
(50) Rezus, Y. L. A.; Bakker, H. J. *Phys. Rev. Lett.* **2007**, *99*, 148301.
(51) Laage, B.; Hynes, J. T. *Science* **2006**, *311*, 832.

(52) Laage, B.; Hynes, J. T. *J. Phys. Chem. B* **2008**, *112*, 14230.
(53) See Supplementary Information.
(54) Laage, B.; Stirnemann, G.; Hynes, J. T. *J. Phys. Chem. B* **2009**, *113*, 2428.
(55) Jana, B.; Pal, S.; Bagchi, B. *J. Phys. Chem. B* **2008**, *112*, 9112.
(56) Halle, B. *Philos. Trans. R. Soc. Lond. B* **2004**, *359*, 1207.
(57) Idrissi, A.; Sokolic, F.; Perera, A. *J. Chem. Phys.* **2000**, *112*, 9479.
(58) Idrissi, A.; Damay, P. *J. Non-Cryst. Solids* **2006**, *352*, 4486.
(59) Mezei, M.; Fleming, P. J.; Srinivasan, R.; Rose, G. D. *Proteins* **2004**, *55*, 502.
(60) López-Llano, J.; Campos, L. A.; Sancho, J. *Proteins* **2006**, *64*, 769.
(61) Shi, Zh.; Chen, K.; Liu, Zh.; Sosnick, T. R.; Kallenbach, N. R. *Proteins* **2006**, *63*, 312.
(62) Chen, K.; Liu, Zh.; Kallenbach, N. R. *Proc. Natl. Acad. Sci. U.S.A.* **2004**, *101*, 15352.
(63) Fleming, P. J.; Fitzkee, N. C.; Mezei, M.; Srinivasan, R.; Rose, G. D. *Protein Sci.* **2005**, *14*, 111.
(64) Kentsis, A.; Mezei, M.; Osman, R. *Proteins* **2005**, *61*, 769.
(65) Shi, Zh.; Olson, C. A.; Rose, G. D.; Baldwin, R. L.; Kallenbach, N. R. *Proc. Natl. Acad. Sci. U.S.A.* **2002**, *99*, 9190.
(66) Yang, S.; Cho, M. *J. Phys. Chem. B* **2007**, *111*, 605.
(67) Young, W. S.; Brooks, C. L., III. *J. Mol. Biol.* **1996**, *259*, 560.
(68) Tran, H. T.; Mao, A.; Pappu, R. V. *J. Am. Chem. Soc.* **2008**, *130*, 7380.

JP9086199